

## Article

# Structural Design and Sealing Performance Analysis of a Nanofluidic Self-Heating Unsealing Rubber Cylinder

Yafei Zhang <sup>1,2,\*</sup> , Taihao Fan <sup>1,2</sup>, Pengbo Zhang <sup>1,2</sup> and Yihua Dou <sup>1,2,\*</sup><sup>1</sup> School of Mechanical Engineering, Xi'an Shiyou University, Xi'an 710065, China<sup>2</sup> Xi'an Key Laboratory of Wellbore Integrity Evaluation, Xi'an Shiyou University, Xi'an 710065, China

\* Correspondence: effyzhang@126.com (Y.Z.); yhdou@vip.sina.com (Y.D.); Tel.: +86-134-8831-1584 (Y.Z.); +86-139-0918-3925 (Y.D.)

**Abstract:** As a crucial component for temporary blocking of layer segments in the segmental fracturing process, bridge plugs are difficult to unseal by conventional methods and may cause major downhole accidents if not handled properly. In this paper, a nanofluidic self-heating unsealing rubber cylinder is designed, which is equipped with a nanofluidic self-heating unsealing sandwich inside the conventional rubber cylinder, consisting of a nanofluidic system and an annular flexible heater. When unsealing, the nanofluidic self-heating unsealing sandwich is heated by the annular flexible heater, and the nanofluidic system can help the bridge plug rubber cylinder shrink in volume and unseal smoothly by the characteristics of heat shrinkage and cold expansion. The nanofluidic system, consisting of porous carbon with an exceptionally large specific surface area and glycerol, serves as a prime example for filling the sandwich layer, and the design parameters calculation was carried out. The sealing performance of the designed nanofluidic self-heating unsealing rubber cylinder was analyzed based on the Mooney–Rivlin principal structure by finite element modeling. The results show that the maximum contact stress between the nanofluidic self-heating unsealing rubber cylinder and the casing wall increases by 9.73%, the compression distance reduces by 24.47%, and the maximum equivalent force decreases by 12.17% on average compared with a conventional rubber cylinder under the same seating load. The designed nanofluidic self-heating unsealing rubber cylinder can satisfy the requirements of pressure-bearing capacity and sealing performance and performs better than a conventional rubber cylinder.

**Keywords:** bridge plug rubber cylinder; nanofluidic self-heating unsealing sandwich; finite element analysis; sealing performance



**Citation:** Zhang, Y.; Fan, T.; Zhang, P.; Dou, Y. Structural Design and Sealing Performance Analysis of a Nanofluidic Self-Heating Unsealing Rubber Cylinder. *Energies* **2023**, *16*, 4890. <https://doi.org/10.3390/en16134890>

Academic Editors: Bin Pan, Xiaopu Wang, Yujie Yuan, Yujing Du and Naser Golsanami

Received: 23 May 2023  
Revised: 19 June 2023  
Accepted: 20 June 2023  
Published: 23 June 2023



**Copyright:** © 2023 by the authors. Licensee MDPI, Basel, Switzerland. This article is an open access article distributed under the terms and conditions of the Creative Commons Attribution (CC BY) license (<https://creativecommons.org/licenses/by/4.0/>).

## 1. Introduction

In the process of oilfield development, bridge plugs, as a temporary downhole sealing tool with the same function as packers [1], are commonly used to seal oil and gas formations to increase oil production and achieve improved reservoir effects [2–4]. When the ambient temperature is high and the bridge plug has been in service for a long time, there are problems of low differential pressure resistance of the rubber cylinder and incomplete recovery because the rubber cylinder relies on rebound force to unseal [5], which causes the rubber cylinder to fail to seal properly and makes it difficult or impossible to raise the string [6,7]. In order to improve the safety of bridge plugs to lift out the string and meet the requirements of downhole sealing construction, researchers have made many attempts to study the structural design of the rubber cylinder. Liu et al. [8] designed a seal structure for a recoverable packer to provide a reference for optimizing the seal performance and pressure-bearing capacity of the packer. Feng et al. [9] developed a graded unsealing long rubber cylinder packer to address the difficulties of unsealing multi-stage packers in finely layered water injection during the extra high water-bearing period. Zhang et al. [10] designed a new dissolvable fracture plug using mechanical and material methods for the

purpose of fracturing slightly deformed cased horizontal wells and achieved unclogging of the wellbore by dissolving the bridge plug during decapping. Swor et al. [11] developed a process which does not require intervention for removal of these tools. The result is self-removing frangible bridges and fracturing plugs that disintegrate from internal explosives and fall downhole into the rathole after service, requiring no removal action. Zachary et al. [12] and Cheng et al. [13] designed a biodegradable bridge plug that eliminates the need for drilling and milling operations after the implementation of segmental fracturing of horizontal wells, improving operational efficiency and greatly reducing operational costs while avoiding damage to casing from drilling and milling operations. Wang et al. [14] optimized the sealing performance and structure of high-pressure and high-temperature packer cartridges and investigated the factors influencing the seal performance of packers in horizontal wells with multi-stage fracturing. Based on the optimal selection of rubber materials, Liu et al. [15] conducted an analysis on the sealing performance of a packer in borehole casing with enlargement/reduction caused by formation. The results indicate that expansion deformation of the casing will result in setting lag or laxity, while shrinkage of the casing will lead to setting advance or even stress failure. The analysis results provide theoretical support for enhancing permanent packer strings and adapting them to complex formations. Wang et al. [16] conducted numerical structural stress analysis on the bridge plug and the packer and optimized the structure of the bell mouth of the rubber cylinder assembly. Hu et al. [17] utilized the hyperelastic-viscoelastic model to investigate the impact of stress relaxation on the sealing performance of rubber materials. Ma et al. [18] conducted a systematic investigation of the contact pressure between packer and tubing under a fixed-displacement load to gain deeper insights into the sealing mechanism of the packer. According to the sealing mechanism of the compression packer rubber, Zhang et al. [19] studied the deformation of rubber between the central tube and casing. Dong et al. [20] examined the impact of temperature loading on both the sealing performance and strength behavior of packer rubber. Zheng et al. [21] conducted a finite element analysis to investigate the impact of temperature and stress relaxation on the performance of packer rubber seal systems. The results indicated that the sealing effectiveness of the packer rubber seal system is significantly influenced by temperature and stress relaxation. However, the current research on structural design of the sealer/bridge plug is mainly focused on material preference and sealing performance and lacks optimal design for unsealing the rubber cylinder.

With the increasing demand for applications and advancements in technology, nanofluidic systems have become a prominent topic of research for new material. On one hand, due to their exceptional mechanical properties, rubber honeycomb core layers filled with nanofluids can restore their original shape after experiencing elastic deformation, providing them with a certain degree of reusability [22]. On the other hand, the nanofluidic system exhibits temperature-dependent volume changes, which result in alterations in its overall volume when subjected to varying temperatures [23].

The present work integrates the nanofluidic system with the bridge plug rubber cylinder to develop a nanofluidic self-heating unsealing rubber cylinder.

The nanofluidic system undergoes volume changes through the addition of an annular nanofluidic self-heating unsealing sandwich within the rubber cylinder. The built-in annular flexible heater in the sandwich heats up the nanofluidic system, causing it to shrink and expand for unsealing of the bridge plug. The automatic unsealing of the rubber cylinder significantly streamlines operations, reduces cycle time, enhances operational efficiency, and mitigates economic losses stemming from seal failure.

## 2. Structure Design and Working Principle

Compared with a conventional rubber cylinder, the nanofluidic self-heating unsealing rubber cylinder is equipped with an additional annular nanofluidic self-heating unsealing sandwich inside the rubber cylinder shown in Figure 1. The three-dimensional skeleton of the sandwich is honeycomb structure and made of ultra-thin thermoplastic polyurethane.

The size of the skeleton can be ignored. The honeycomb is filled with the nanofluidic system. An annular flexible heater is arranged at the top and inside the sandwich, which is a PE-etched foil with a thickness of 0.13 mm. The heater is driven by a power supply located on the bridge plug.

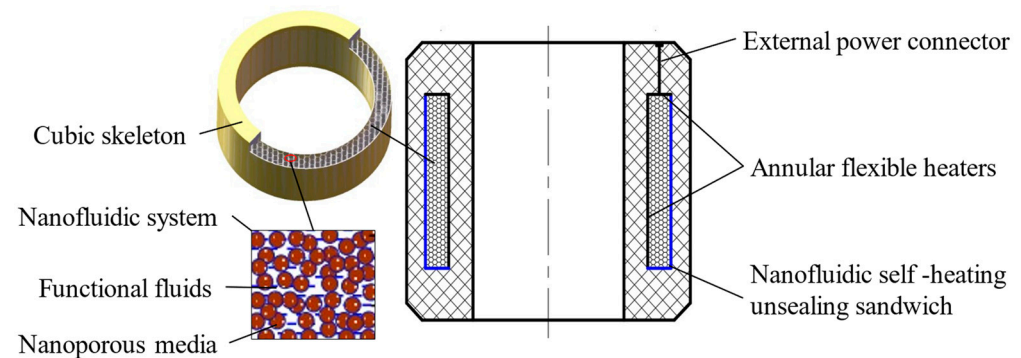


**Figure 1.** Schematic diagram of the structure of nanofluidic self-heating unsealing rubber cylinder.

The nanofluidic system is the core working unit of the rubber cylinder. The nanofluidic system consists of a functional liquid and a nanoporous medium. When the nanoporous medium and functional liquid are not wettable to each other, the functional liquid will not spontaneously enter the hydrophobic nanopore channels under interfacial tension until the pressure of tens or even hundreds of MPa is applied on the functional liquid [24]. Since both interfacial tension  $\gamma_{sl}$  and contact angle  $\alpha$  are functions of the liquid temperature, the critical infiltration pressure  $p_{in}$  is influenced by temperature [25]. As shown in Figure 2a, the surface tension  $\gamma_{sl}$ , critical infiltration pressure  $p_{in}$ , and infiltration volume  $\Delta V$  of the nanofluidic system change with variation in temperature. As the temperature increases, both the interfacial tension  $\gamma_{sl}$  and the critical infiltration pressure  $p_{in}$  decrease. If the applied external load is lower than the current critical infiltration pressure  $p_{in}$ , an increase in system temperature can reduce both interfacial tension  $\gamma_{sl}$  and current critical infiltration pressure  $p_{in}$  [26,27]. This results in functional liquid spontaneously penetrating into the nanopore channels without any change to the external load. The change in infiltration volume  $\Delta V$  of the entire system increases while the overall volume of the nanofluidic system decreases. Based on this principle, temperature adjustment can be used as a valve to drive functional liquid into the channel of porous medium, thereby regulating the volume of the sealer rubber cylinder and assisting in shrinkage and unsealing.

Figure 2b shows the schematic diagram of the working principle of nanofluidic self-heating unsealing sandwich. The  $T_{low}$  curve represents the situation of the nanofluidic self-heating unsealing rubber cylinder during normal service. When the temperature of the sandwich is  $T_{low}$ , the critical infiltration pressure of the nanofluidic system is  $p_{in,low}$ , and the infiltration volume of the functional liquid into the pore channel of the porous medium is  $\Delta V_{low}$ . The rubber cylinder is in a sealed state.

The  $T_{high}$  curve represents the situation of the nanofluidic self-heating unsealing rubber cylinder in the unsealing process. When the nanofluidic sandwich layer is heated by the internal annular heater, the temperature of the sandwich layer increases from  $T_{low}$  to  $T_{high}$ , and the interfacial tension  $\gamma_{sl}$  between the solid and liquid phases of the nanofluidic system decreases. Therefore, the critical infiltration pressure of the nanofluidic system decreases from  $p_{in,low}$  to  $p_{in,high}$ . Once the critical infiltration pressure decreases, the functional liquid originally blocked outside the pore can flow into the channel of porous medium. Thus, the infiltration volume increases from  $\Delta V_{low}$  to  $\Delta V_{high}$ , which macroscopically leads to the shrinkage of the sandwich volume. The reduction in the volume of the nanofluidic self-heating unsealing rubber cylinder, denoted as  $\Delta V_{low} - \Delta V_{high}$ , facilitates bridge plug unsealing and enhances the success rate of this process.

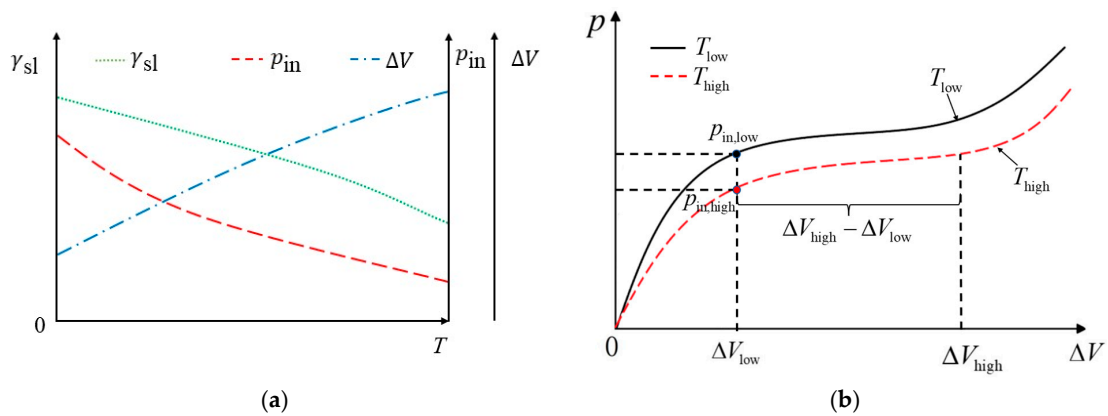


**Figure 2.** Schematic diagram of the parameters of the nanofluidic system varying with temperature: (a) variation curves of surface tension, critical infiltration pressure, and infiltration volume with temperature for nanofluidic system; (b) schematic diagram of the working principle of nanofluidic self-heating unsealing sandwich.

**3. Size Design Method and Calculation Case Study**

*3.1. Design Method of Nanofluidic Self-Heating Unsealing Sandwich Size*

The nanofluidic self-heating unsealing sandwich is the core device to achieve self-heating unsealing of the rubber cylinder. Before design, the target volume auxiliary shrinkage of the rubber cylinder  $V_{sh}$  needs to be determined according to the application requirements. Assuming that the target volume auxiliary shrinkage of the rubber cylinder  $V_{sh}$  is  $k$  times the volume of the rubber cylinder when it is fully sealing set, the target volume auxiliary shrinkage of the rubber cylinder can be calculated by equations as follows:

$$V_{sh} = k\% \times \frac{\pi}{4} (D_{tn}^2 - D_{jn}^2) (H - H_Z) \tag{1}$$

where  $k$  is the percentage of volume shrinkage when the rubber cylinder is auxiliary unsealed, equal to the auxiliary shrinkage of rubber cylinder target volume  $V_{sh}$  divided by the volume when the tube is completely set, %;  $H$  is the height of the rubber cylinder, mm;  $H_Z$  is the seating route, mm;  $D_{tn}$  is the inner diameter of the casing, mm; and  $D_{jn}$  is the inner diameter of the rubber cylinder, mm. Related dimensional parameters are shown in Figure 3.

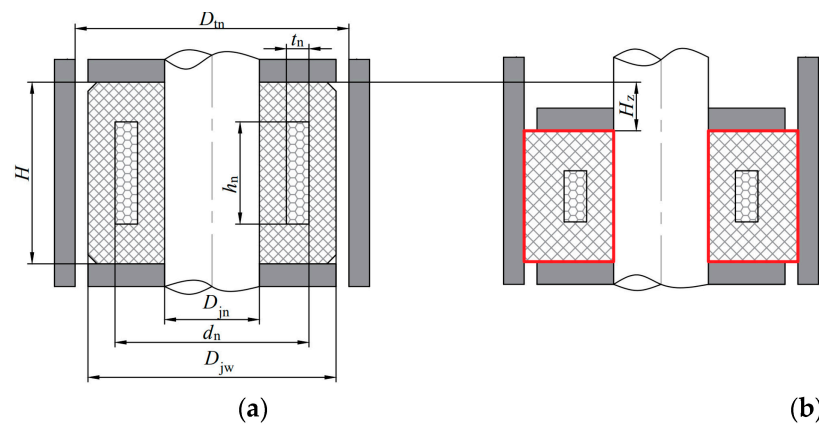


**Figure 3.** Schematic diagram of nanofluidic self-heating unsealing bridge plug rubber cylinder seating structure: (a) schematic diagram of the structure of the nanofluidic self-heating unsealing bridge plug rubber cylinder before sitting and sealing; (b) schematic diagram of the structure of the nanofluidic self-heating unsealing bridge plug rubber cylinder after sitting and sealing (The red frame indicates the shape of the rubber cylinder after it is fully seated.).

According to the working principle of the nanofluidic self-heating unsealing rubber cylinder, the target auxiliary volume shrinkage of the rubber cylinder is equal to the volume variation after warming the sandwich layer. Since the pore size of the porous medium used in practice is not uniform and some of the pores may collapse, the functional liquid cannot enter all the channels.  $\alpha$  is proposed as the pore quality factor of the nanoporous medium to describe the effective pore volume of the porous medium. Then the relationship between the nanoporous medium mass  $m_p$  and the target auxiliary volume shrinkage of the rubber cylinder  $V_{sh}$  can be described by equations as follows:

$$\alpha \Delta V_{sh} = m_p V_{acc} \quad (2)$$

where  $V_{acc}$  is the pore volume per unit mass of nanoporous medium,  $m^3/kg$ .

Assuming that the functional liquid and the nanoporous medium are mixed with a mass ratio of  $m : n$ , then the mass  $m_g$  of the functional liquid can be calculated by equations as follows:

$$m_g = m_p m / n \quad (3)$$

Moreover, the volume of nanoporous medium  $V_p$  can be calculated from the unit mass of pore volume  $V_{acc}$ , the mass of nanoporous medium  $m_p$  and the porosity  $\varphi$  as follows:

$$V_p = m_p V_{acc} / \varphi \quad (4)$$

where  $\varphi$  is the porosity, characterizing the ratio of the volume occupied by pores in a nanoporous medium to the total volume of the porous material.

The volume  $V_n$  of the nanofluidic system is the sum of the nanoporous medium volume  $V_p$  and the functional liquid volume  $V_g$  in the sandwich. The  $V_n$  can be calculated as follows:

$$V_n = V_g + V_p = \frac{m}{n} \frac{\alpha \Delta V_{sh}}{V_{acc} \rho_g} + m_p V_{acc} / \varphi \quad (5)$$

where  $\rho_g$  is the density of the functional liquid,  $kg/m^3$ .

The thickness  $t_n$  of the sandwich is calculated based on the total volume of the nanofluidic system sandwich. Based on the application requirements, assume that the outer diameter of the nanofluidic system self-heating unsealing sandwich is  $d_n$ , and the sandwich height is  $h_n$ . Then  $V_n$  can be obtained as follows.

$$V_n = \frac{\pi}{4} h_n [d_n^2 - (d_n - 2t_n)^2] \quad (6)$$

where  $d_n$  is the outer diameter of the sandwich, mm;  $h_n$  is the height of the sandwich, mm;  $t_n$  is the thickness of the sandwich, mm.

Transforming Equation (6), the thickness  $t_n$  of the sandwich is:

$$t_n = \frac{1}{2} (d_n - \sqrt{d_n^2 - \frac{4}{\pi h_n} V_n}) \quad (7)$$

where  $h_n$  is the sandwich height, in order to ensure the pressure-bearing performance, it is recommended to select  $60\% \pm 5\%$  of the height of the rubber cylinder; and  $d_n$  is the outer diameter of the sandwich, which can be adjusted according to the size of the volume of the nanofluidic system, with range of  $D_{jw} - 1/3 \sim 1/6(D_{jw} - D_{jn})$ , where  $D_{jw}$  is the outer diameter of the rubber cylinder, mm.

### 3.2. Case Study of Sandwich Size Calculation

A kind of expanding rubber cylinder is utilized in this study. The parameters of the expanding bridge plug are determined as follows [28]. The applicable sleeving is 5.5 inches (139.7 mm), and the working pressure is set to 50 MPa. The outer diameter of the rubber cylinder is 110 mm, the inner diameter is 68 mm, and the height is 80 mm. The end face inclination of the rubber cylinder is  $45^\circ$ . The allowable gap between the rubber cylinder

and the sleeving is 5.7 mm, and the route of sealing set is 22.4 mm. Based on these design parameters mentioned above, a nanofluidic self-heating unsealing sandwich is constructed inside the rubber cylinder.

The nanofluidic system mixture encapsulated inside the rubber cylinder sandwich is configured according to the service environment of the bridge plug in the rubber cylinder. The porous carbon has large specific surface area, good gas–liquid permeability, adjustable pore structure, and favorable thermal stability. Therefore, it was selected as the nanoporous medium in the nanofluidic system. Its physical properties are shown in Table 1. The functional liquid is glycerol, which has a high boiling point, is not volatile, has high viscosity, and is not easy to crystallize. The nanofluidic system is configured by mixing the porous carbon with glycerol in the ratio of 4 : 1 by mass and filling into the designed self-heating unsealing gel rubber cylinder nanofluidic sandwich.

**Table 1.** Physical properties of porous carbon with ultra-large specific surface area.

Parameters	Numerical Value
Specific surface area/m <sup>2</sup> ·g <sup>-1</sup>	3500
Aperture/nm	2
Pore volume per unit mass/cm <sup>3</sup> ·g <sup>-1</sup>	1.6
Pore quality factor	1.5
Porosity	0.5

According to the application requirement, 10% of the volume of the rubber cylinder with completely sealed set is taken as the target auxiliary shrinkage volume. The target auxiliary shrinkage volume of the nanofluidic self-heating unsealing rubber cylinder is  $1.268 \times 10^{-5} \text{ m}^3$  calculated by Equation (1). The mass of porous carbon is 12 g obtained by Equation (2), and the mass of glycerol is 48 g by substituting the mass of porous carbon into Equation (3). The density of glycerol is  $1260 \text{ kg/m}^3$ , thus the volume of glycerol is obtained for  $3.774 \times 10^{-5} \text{ m}^3$ . The volume of porous carbon is  $3.804 \times 10^{-5} \text{ m}^3$  obtained by Equation (4). If the volume of the nanofluidic system is the volume sum of glycerol and porous carbon, then the volume of the nanofluidic system is  $7.578 \times 10^{-5} \text{ m}^3$  according to Equation (5). The sandwich height  $h_n$  is taken as 45 mm calculated from 55% of the rubber cylinder height. The outer diameter of the sandwich  $d_n$  is taken as 98 mm according to  $D_{jw} - 1/3(D_{jw} - D_{jn})$ , and the thickness of the sandwich is obtained as 10 mm by substituting  $d_n$  into Equations (6) and (7).

#### 4. Analysis of Sealing Performance

##### 4.1. Finite Element Modeling

According to the working principle of the bridge plug, the components of the bridge plug are simplified as pressure ring, central tube, nanofluidic self-heating unsealing sandwich, glue rubber cylinder, and sleeve. The structural parameters of the rubber cylinder for the bridge plug are presented in Table 2, which is utilized in the case analysis of nanofluidic self-heating unsealing rubber cylinder as discussed in Section 3.2.

**Table 2.** Structural parameters of the rubber cylinder.

Parameters	Height/mm	Inner Diameter/mm	Outer Diameter/mm
Casing	100	121.4	139.7
Center tube	100	42	68
Pressure ring	10	68	110
Rubber cylinder	80	68	110
Nanofluidic self-heating unsealing sandwich	45	88	98

Based on the structural parameters of the bridge plug casing in Table 2, a finite element analysis model of the conventional casing and the nanofluidic self-heating unsealing casing is constructed as shown in Figure 4. The material of the casing, center tube, and upper and lower compression rings are defined as structural steel, with elastic modulus  $E = 2.06 \times 10^5$  MPa and the Poisson's ratio  $\mu = 0.25$  [28]. The mechanical characteristics of the nanofluidic system in the sandwich are described by the model of elastic deformation, plastic crushing, and densification [29]. The material of the rubber cylinder was selected as hydrogenated nitrile rubber except for the sandwich. The Mooney-Rivlin intrinsic model was used in the simulation work with parameters set as:  $C_{10} = 1.926$  MPa,  $C_{01} = 0.963$  MPa, elastic modulus  $E = 17.33$  MPa, Poisson's ratio  $\mu = 0.3$ , and friction coefficient as  $f = 0.3$  [30]. The rubber cylinder was meshed with hexahedral cells, and the rest of the geometrical model was meshed with tetrahedral cells.

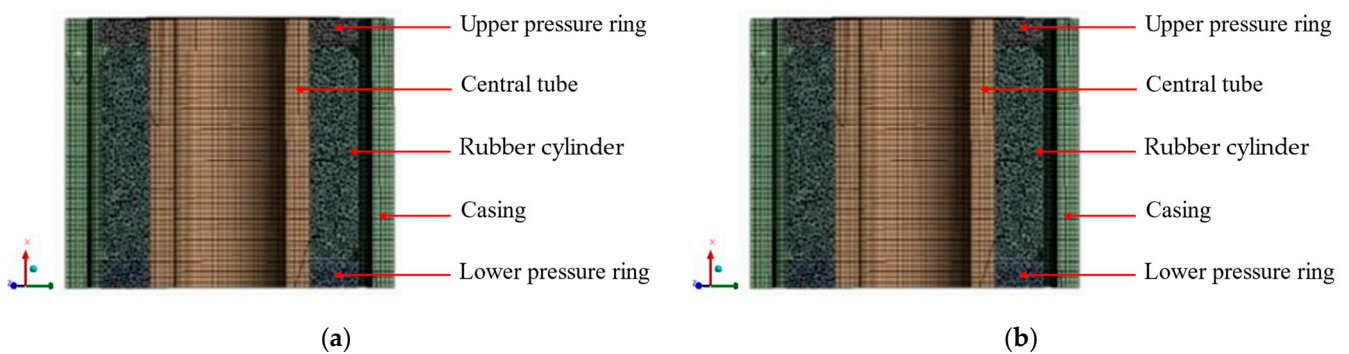
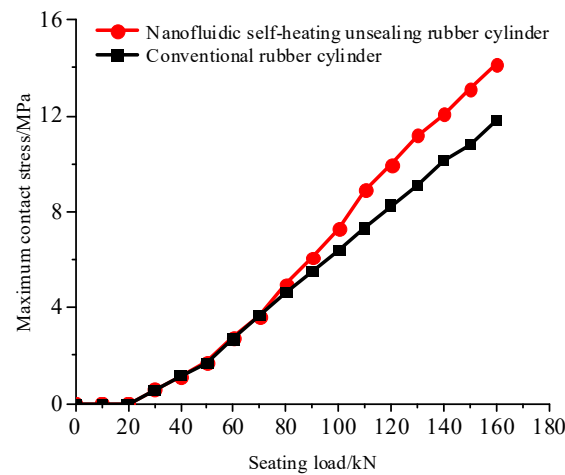


**Figure 4.** Finite element analysis model of conventional rubber cylinder and nanofluidic self-heating unsealing rubber cylinder. (a) Conventional rubber cylinder; (b) nanofluidic self-heating unsealing rubber cylinder.

#### 4.2. Analysis of Simulation Results

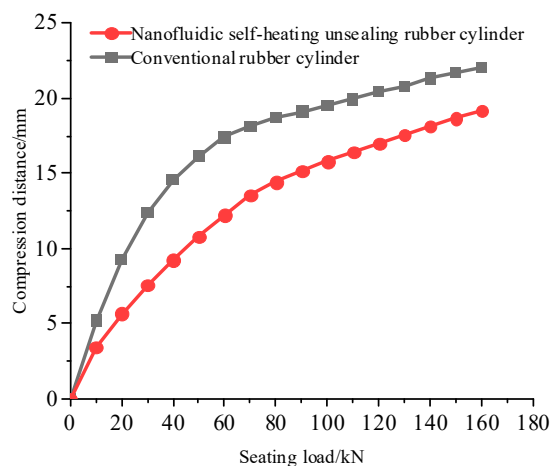
The maximum contact stresses between the conventional rubber cylinder and the nanofluidic self-heating unsealing rubber cylinder under different seating loads were compared to verify the sealing performance of the latter system.

Figure 5 shows the maximum contact stresses between the conventional rubber cylinder and the nanofluidic self-heating unsealing one under different seating loads. With the increase in seating load, the maximum contact stresses of rubber cylinders in both cases increase gradually, which is consistent with findings reported in the literature [31]. When the seating load ranges from 0 to 70 kN, the maximum contact stress trends of both types of rubber cylinders exhibit a similar pattern. Due to the low initial seating load on the rubber cylinder, the degree of sandwich deformation in the nanofluidic self-heating unsealing rubber cylinder is negligible, resulting in a small maximum contact stress on the casing wall. When the seating load is greater than 70 kN, the maximum contact stress of the nanofluidic self-heating unsealing rubber cylinder is always larger than that of the conventional one. This is attributed to the nanofluidic self-heating unsealing rubber cylinder, which features a unique three-dimensional honeycomb structure containing an encapsulated nanofluidic system fluid within the honeycomb. Compared to conventional rubber cylinders, it exhibits an enhanced degree of deformation and pressure-bearing capacity [32] and demonstrates higher maximum contact stress with the casing wall under the same seating load. The maximum contact stress of the nanofluidic self-heating unsealing rubber cylinder exhibits an average increase of 9.73% compared to that of the conventional rubber cylinder, indicating its superior adaptability to normal operation conditions in well bridge plugs.



**Figure 5.** Variation curves of the maximum contact stress compared.

The compression distance of the bridge plug under different seating loads serves as a crucial indicator for evaluating its sealing performance, reflecting the compression rate and deformation state of the rubber cylinder under varying loads [33]. By simulating the seating process of bridge plugs, the compression distances of the conventional rubber cylinder and the nanofluidic self-heating unsealing rubber cylinder are compared under different seating loads in Figure 6.



**Figure 6.** Variation curves of compression distance.

The deformation of rubber cylinders gradually increases and the slope of the curve gradually decreases as the seating load increases in both cases. This is because the cylinder undergoes free deformation at the initial stage, resulting in significant changes in compression distance. The aforementioned finding is consistent with the results reported in the literature [34]. With the further increase in load, it undergoes compaction and compression with increasing difficulty, resulting in a reduction in compression distance. Additionally, it is noteworthy that the conventional rubber cylinder consistently exhibits a greater compression distance than that of the nanofluidic self-heating unsealing rubber cylinder. By incorporating the honeycomb skeleton with exceptional compressive strength, the rubber cylinder exhibits superior pressure-bearing performance [35]. The compression distance of the nanofluidic self-heating unsealing rubber cylinder is reduced by 24.47% on average compared with the compression distance of the conventional one. This indicates that the nanofluidic self-heating unsealing rubber cylinder has a higher compression capacity and a smaller deformation pattern, its contact length with the casing is longer, and the seal is better under the same seating load.

The maximum mises stress of the rubber cylinder affects its pressure resistance and service life [36]. The maximum mises stresses of the conventional rubber cylinders and the nanofluidic self-heating unsealing ones under different seating loads were extracted and plotted in Figure 7.

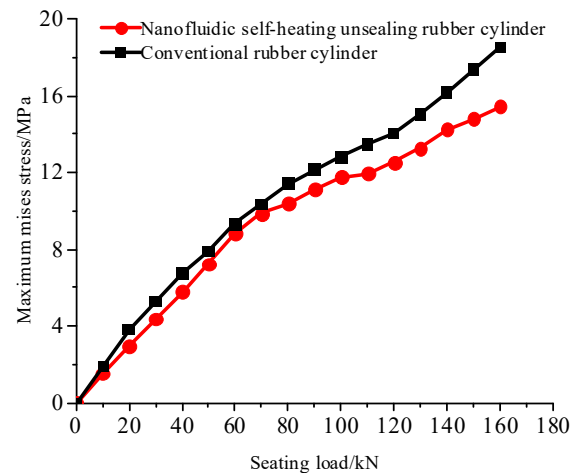


**Figure 7.** Variation curve of maximum equivalent stress.

As shown in Figure 7, the maximum mises stress enlarges with the increase in seating load in both cases, which is in accordance with the research results in the literature [37]. Under the same seating load, the maximum mises stress of the nanofluidic self-heating unsealing rubber cylinder is 12.17% lower than that of the conventional one on average. This demonstrates that the sandwich structure incorporated in the nanofluidic self-heating unsealing rubber cylinder effectively alleviates maximum mises stress. According to reports, a lower mises stress level corresponds to higher compressive strength, which in turn reduces the risk of tearing and prolongs service life [38]. Therefore, the use of nanofluidic self-heating unsealing rubber cylinders can effectively mitigate the risk of tearing.

## 5. Conclusions

In this paper, a nanofluidic self-heating unsealing rubber cylinder is proposed, which incorporates a nanofluidic self-heating unsealing sandwich that contracts upon exposure to heat and facilitates the unsealing of bridge plugs. Combined with the working principle of a nanofluidic self-heating unsealing sandwich, a design methodology for the sandwich is established. Taking nanofluidic system composed of porous carbon and glycerol as an example filling formulation of the nanofluidic self-heating unsealing sandwich, the feasibility of size design for nanofluidic self-heating unsealing rubber cylinder sandwiches is verified, and the sealing performance of nanofluidic self-heating unsealing rubber cylinders is analyzed. Compared to conventional rubber cylinders, the maximum contact stress between nanofluidic self-heating unsealing ones and the casing wall is increased by 9.73% on average, the compression distance is reduced by 24.47% on average, and the maximum equivalent stress is reduced by 12.17% on average. The designed nanofluidic self-heating unsealing rubber cylinder exhibits superior pressure resistance and sealing properties compared to conventional rubber cylinders, meeting the requirements of its intended application.

By adjusting the nanofluidic system formula in self-heating unsealing sandwiches, rubber cylinders suitable for various application conditions can be obtained to address engineering issues arising from bridge plug rubber cylinder failure due to unsealing and shrinking.

**Author Contributions:** Conceptualization, Y.Z. and Y.D.; methodology, Y.Z. and T.F.; validation, T.F. and P.Z.; formal analysis, Y.Z. and T.F.; investigation, P.Z.; resources, P.Z.; data curation, T.F.; writing—original draft preparation, Y.Z.; writing—review and editing, Y.D.; supervision, Y.D.; project administration, Y.D.; funding acquisition, Y.Z. All authors have read and agreed to the published version of the manuscript.

**Funding:** This research study was funded by the National Natural Science Foundation of China (grant No. 51974246 and 51806173) and the Innovative Talent Promotion Program “Young Science and Technology Star Project” of Shaanxi Province of China (grant No. 2021KJXX-40).

**Data Availability Statement:** Not applicable.

**Conflicts of Interest:** The authors declare no conflict of interest.

## References

- Pan, L.; Oldenburg, C.M. Mechanistic modeling of CO<sub>2</sub> well leakage in a generic abandoned well through a bridge plug cement-casing gap. *Int. J. Greenh. Gas Control* **2020**, *97*, 103025. [[CrossRef](#)]
- Lei, Q.; Xu, Y.; Cai, B.; Guan, B.; Wang, X.; Bi, G.; Li, H.; Li, S.; Ding, B.; Fu, H.; et al. Progress and prospects of horizontal well fracturing technology for shale oil and gas reservoirs. *Pet. Explor. Dev.* **2022**, *49*, 191–199. [[CrossRef](#)]
- Novy, R.A. Pressure Drops in Horizontal Wells: When Can They Be Ignored? *SPE Res. Eng.* **1995**, *10*, 29–35. [[CrossRef](#)]
- Ratterman, E.E.; Augustine, J.R.; Voll, B.A. New Technology Applications to Increase Oil Recovery by Creating Uniform Flow Profiles in Horizontal Wells: Case Studies and Technology Overview. In Proceedings of the International Petroleum Technology Conference, Doha, Qatar, 21–23 November 2005; p. 10177.
- Han, Y.; Liu, Z.; Zhou, H.; Zhang, P.; Guo, M.; Zhan, H.; Ren, Z.; Sun, X. Research of Unthrottled Self-unsetting Packer and Technology String. *Mech. Eng.* **2019**, *339*, 70–73. (In Chinese)
- Hu, Y.; Yang, K.; Li, J.; Yang, J.; Wang, C.; Miao, Y.; Qiao, R. Research and Application of Multistage Fracturing Self-releasing Packer and Tubing String. *Pet. Mach.* **2017**, *45*, 83–86. (In Chinese)
- Wang, J.; Jia, H.; You, J. Performance Analysis of Soluble Bridge Plug Materials for Fracturing in Unconventional Oilfields. *Math. Probl. Eng.* **2022**, *2022*, 1911173. [[CrossRef](#)]
- Liu, Y.; Lian, Z.; Chen, J.; Kuang, S.; Mou, Y.; Wang, Y. Design and Experimental Research on Sealing Structure for a Retrievable Packer. *Shock. Vib.* **2020**, *2020*, 7695276. [[CrossRef](#)]
- Feng, Y.; Wu, K. Structure and Performance analysis of gradual Releasing long Tubing packer. *Oil Field Equip.* **2015**, *44*, 79–82.
- Zhang, P.; Pu, C.; Pu, J.; Wang, Z. Study and Field Trials on Dissolvable Frac Plugs for Slightly Deformed Casing Horizontal Well Volume Fracturing. *ACS Omega* **2022**, *7*, 10292–10303. [[CrossRef](#)]
- Swor, L.; Sonnefeld, A. Self-Removing Frangible Bridge and Fracture Plugs. In Proceedings of the SPE Annual Technical Conference and Exhibition, San Antonio, TX, USA, 24–27 September 2006.
- Zachary, W.; Porter, J.; Fripp, M.; Vargus, G. Cost and Value of a Dissolvable Frac Plug. In Proceedings of the SPE/ICoTA Coiled Tubing and Well Intervention Conference and Exhibition, Houston, TX, USA, 21–22 March 2017.
- Cheng, K.; Shang, L.; Li, H.; Peng, B.; Li, Z. A novel degradable sealing material for the preparation of dissolvable packer rubber barrel. *J. Macromol. Sci. A* **2023**, *60*, 201–216. [[CrossRef](#)]
- Wang, X.; Zhang, X.; Chen, S. Sealing properties and structure optimization of packer rubber under high pressure and high temperature. *Pet. Sci.* **2019**, *16*, 632–644.
- Liu, Z.; Li, S.; Zhang, L.; Wang, F.; Wang, P.; Han, L.; Ma, Y.; Zhang, H. Analysis of Sealing Mechanical Properties of Fracturing Packer Under Complex Conditions. *J. Fail. Anal. Prev.* **2019**, *19*, 1569–1582. [[CrossRef](#)]
- Wang, L.; Sheng, X.; Sheng, J. Analysis of the Pressure Expansion of Bridge Plug Tools and Packers by Equivalent Material Method. *J. Phys. Conf. Ser.* **2019**, *1187*, 032052. [[CrossRef](#)]
- Hu, G.; Liu, Y.; Wang, G.; Wu, W.; Xu, Z.; Shen, K. Research on the Influence of Stress Relaxation on the Sealing Performance of the Packer under HTHP. *J. Fail. Anal. Prev.* **2022**, *22*, 841–857. [[CrossRef](#)]
- Ma, W.; Qu, B.; Guan, F. Effect of the friction coefficient for contact pressure of packer rubber. *Proc. Inst. Mech. Eng. Part C J. Mech. Eng. Sci.* **2014**, *228*, 2881–2887. [[CrossRef](#)]
- Zhang, F.; Jiang, X.; Wang, H.; Song, N.; Chen, J.; Duan, J. Mechanical analysis of sealing performance for compression packer. *Mech. Ind.* **2018**, *19*, 309–319. [[CrossRef](#)]
- Dong, L.; Li, K.; Zhu, X.; Li, Z.; Zhang, D.; Pan, Y.; Chen, X. Study on high temperature sealing behavior of packer rubber tube based on thermal aging experiments. *Eng. Fail. Anal.* **2020**, *108*, 104321. [[CrossRef](#)]
- Zheng, X.; Li, B. Study on sealing performance of packer rubber based on stress relaxation experiment. *Eng. Fail. Anal.* **2021**, *121*, 105692. [[CrossRef](#)]
- Feng, G.; Li, S.; Xiao, L.; Song, W. Energy absorption performance of honeycombs with curved cell walls under quasi-static compression. *Int. J. Mech. Sci.* **2021**, *210*, 106746. [[CrossRef](#)]
- Xu, B.; Qiao, Y.; Park, T.; Tak, M.; Zhou, Q.; Chen, X. A conceptual thermal actuation system driven by interface tension of nanofluids. *Energy Environ. Sci.* **2011**, *4*, 3632–3639. [[CrossRef](#)]

24. Liu, L.; Zhao, J.; Yin, C.; Culligana, P.J.; Chen, X. Mechanisms of water infiltration into conical hydrophobic nanopores. *Phys. Chem. Chem. Phys.* **2009**, *11*, 6520–6524. [[CrossRef](#)]
25. Li, W. Further explanation of the direction of gas-liquid interfacial tension in the derivation of Young's equation. *Chem. Higher Educ.* **2016**, *33*, 84–94. (In Chinese)
26. Han, A.; Qiao, Y. A volume-memory liquid. *Applied Physics Letters. Appl. Phys. Lett.* **2007**, *91*, 173123. [[CrossRef](#)]
27. Zhang, Y.; Li, N.; Lou, R.; Zhang, Y.; Zhou, Q.; Chen, X. Experimental study on thermal effect on infiltration mechanisms of glycerol into ZSM-5 zeolite under cyclic loadings. *J. Phys. D Appl. Phys.* **2016**, *49*, 025303. [[CrossRef](#)]
28. Zheng, C.; Zheng, X.; Qin, J.; Liu, P.; Aibaibu, A.; Liu, Y. Nonlinear finite element analysis on the sealing performance of rubber packer for hydraulic fracturing. *J. Nat. Gas. Sci. Eng.* **2021**, *85*, 103711. [[CrossRef](#)]
29. Zhang, Y.; Liang, J.; Luo, R.; Min, S.; Dou, Y. Application Characteristics of Zeolite-Based Stuffing for Nanofluidic Packer Rubber. *Energies* **2022**, *15*, 7962. [[CrossRef](#)]
30. Liu, Y.; Qian, L.; Zou, J.; Xia, C.; Lian, Z. Study on failure mechanism and sealing performance optimization of compression packer. *Eng. Fail. Anal.* **2022**, *136*, 106176. [[CrossRef](#)]
31. Hu, G.; Zhang, P.; Wang, G.; Zhang, M.; Li, M. The influence of rubber material on sealing performance of packing element in compression packer. *J. Nat. Gas Sci. Eng.* **2017**, *38*, 120–138. [[CrossRef](#)]
32. Zhang, Y.; Min, S.; Wang, H.; Gao, M.; Dou, Y. Analysis on loading capacity of first-order honeycomb skeleton of nanofluidic packer rubber. *Pet. Mach.* **2022**, *50*, 73–78. (In Chinese)
33. Zhang, Z.; Zhu, X.; Xu, J. Structural parameters optimization of compression packer rubber based on orthogonal test. *Nat. Gas Ind.* **2019**, *39*, 80–84. (In Chinese)
34. Liu, J.; Deng, K.; Liu, S.; Yan, X.; Li, L.; Zou, D.; Lin, Y. Mechanical Behavior and Structure Optimization of Compressed PHP Packer Rubber. *J. Mater. Eng. Perform.* **2021**, *30*, 3691–3704. [[CrossRef](#)]
35. Zhang, Y.; Liang, J.; Liu, J.; Xiao, H.; Dou, Y. Energy absorption characteristics of honeycomb structure of nanofluidic packer rubber under coplanar compression. *Pet. Mach.* **2022**, *50*, 89–95. (In Chinese)
36. Jiao, K.; Yun, F.; Yan, Z.; Wang, G.; Jia, P.; Wang, L.; Liu, D.; Hao, X. Optimization and Experimental Study of the Subsea Retractable Connector Rubber Packer Based on Mooney-Rivlin Constitutive Model. *J. Mar. Sci. Eng.* **2021**, *9*, 1391. [[CrossRef](#)]
37. Hu, G.; Wang, M.; Wang, G.; He, X. Research on the Influence of Spacer Ring on the Sealing Performance of Packing Element used in Compression Packer. *J. Fail. Anal. Prev.* **2021**, *21*, 1605–1621. [[CrossRef](#)]
38. Li, B.; Lu, D.; Zhang, Z. Analysis of mechanical properties of wave packer rubber. *J. Appl. Mech.* **2018**, *35*, 828–833. (In Chinese)

**Disclaimer/Publisher's Note:** The statements, opinions and data contained in all publications are solely those of the individual author(s) and contributor(s) and not of MDPI and/or the editor(s). MDPI and/or the editor(s) disclaim responsibility for any injury to people or property resulting from any ideas, methods, instructions or products referred to in the content.